AD NUMBER

AD479297

NEW LIMITATION CHANGE

TO

Approved for public release, distribution unlimited

FROM

Distribution: Further dissemination only as directed by Office of Naval Research, Arlington, Va 22217-0000; Oct 1965 or higher DoD authority.

AUTHORITY

ONR ltr 27 Jul 1971

PRESSURE MEASUREMENT ON FLAPPED HYDROFOILS IN CAVITY FLOWS AND WAKF FLOWS[1)]

by

M. C. Meijer[2)]

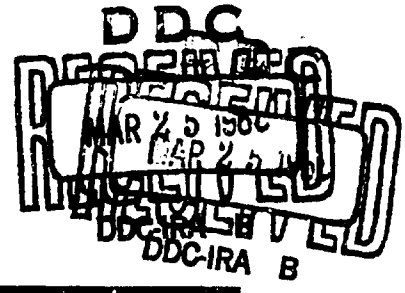

HYDRODYNAMICS LABORATORY

KÁRMÁN LABORATORY OF FLUID MECHANICS AND JET PROPULSION

CALIFORNIA INSTITUTE OF TECHNOLOGY

PASADENA, CALIFORNIA

Hydrodynamics Laboratory
Kármán Laboratory of Fluid Mechanics and Jet Propulsion
California Institute of Technology
Pasadena, California

PRESSURE MEASUREMENT ON FLAPPED HYDROFOILS IN CAVITY FLOWS AND WAKE FLOWS [1)]

by

M. C. Meijer [2)]

1) This work was carried out under the Bureau of Ships General Hydrodynamics Research Program, Administered by the David Taylor Model Basin, Office of Naval Resea. ch Contract Nonr-220(52).

2) Senior Research Engineer, California Institute of Technology, Pasadena, California, 1962-64. Present address: Shipbuilding Laboratory of the Technological University of Delft, Netherlands.

Report No. E-133.2 October 1965

SUMMARY

The purpose of the present experiments is to obtain a detailed information about the flow field, such as the pressure distribution, at the surface of a flapped hydrofoil in full cavity or wake flows. The model and the experimental procedure are described. The experimental results obtained have been used to compare with the theoretical predictions, to investigate the tunnel wall effect and to estimate the viscous effect at a sharp corner. An empirical method for correcting the tunnel wall effect is developed here, the validity of which is supported by tests with models of three different sizes. An appreciable viscous effect has been found near the hinge of a deflected flap. Except for this effect, the theory and experiments are found to be in good agreement.

Introduction

In the classical theory of free streamline flows and its application to cavity and wake phenomena, it is well known that even in the limiting case of infinite cavities, the numerical calculation of the solution for arbitrary obstacles presents much difficulties, as has been extensively discussed in some recent survey literatures (1), (2). For the general case of finite cavities, the problem is further complicated by an additional parameter, namely the cavitation number. In 1962 Wu (3) introduced a simple wake model and developed a theory for plane wake and cavity flows past an inclined flat plate at an arbitrary cavitation number. This theory was subsequently extended by Wu and Wang (4) to the general case of arbitrary body form and arbitrary cavitation number. The original theory has been found in good agreement with the experimental results of Fage and Johansen (5) who measured the pressure distribution over a flat plate, inclined in a separated flow in a windtunnel. The total force coefficients predicted by this theory also compare satisfactorily with several water tunnel experimental results. In order to establish the theory fully, it is still important to check experimentally with the detailed flow field, such as the pressure distribution over the body surface, for some typical cases of arbitrary body form. Such comparisons may clarify the validity of the theoretical model and the simplifying assumptions of neglecting the effects of viscosity and gravity.

From the viewpoint of experimental activities, it may be pointed out that in most of the previous model tests of cavity flows in water tunnels only the forces and moments were recorded, whereas detailed surveys of the pressure field over the body surface are indeed very scarce. Furthermore the present technique of using water tunnels for cavity flow studies is also handicapped by a lack of a well established method for wall corrections so that the experimental errors can be precisely eliminated. Such a method for the most general condition should be extremely valuable for the future experimental purposes.

In view of the ever increasing scope of applications of cavity flow

theory, such as supercavitating hydrofoil watercrafts, stalled wing performance in VTOL operations, supercavitating propellers and cascades, a thoroughly verified theory for ready use and a well defined experimental interpretation are both of utmost importance. Furthermore in hydrofoil applications, adoption of flaps or other load modulators as control devices is necessary and a good knowledge of supercavitating flaps is still much in need. For these reasons it has become the main purpose of this experimental program to choose the supercavitating hydrofoil with flaps as a concrete case for investigating the validity of the theory and developing a wall correction method.

From the earlier data obtained in the course of this investigation, it was first found that the local pressure coefficient is more sensitive to wall effect than the force coefficients. Consequently a correct method for estimating the wall effect is necessary for a meaningful interpretation of the data. By using several geometrically similar models of three different sizes, an empirical method for wall correction is developed here, by which the experimental data can be reduced consistently to a single result, insensitive to the model scale, thus providing a reliable correlation to the theoretical case of unbounded flows. In other words, the present method is supported at least by this experiment for the different model scales tested. After the data were so reduced, the theory is found to be in good agreement with the experiment except in a small region near the flap hinge, where the influence of viscosity is revealed by these experiments. From the over-all result it may be concluded that primary success has been achieved for both of the two main purposes of this study.

The Hydrofoil Model

The main purpose of this experimental program is to make a detailed survey of the flow field near the hydrofoil-cavity system. Such information is not only valuable for verifying the theoretical model used to obtain the solution, but is also useful for investigating the related problems of wall effect and any possible effect due to viscosity. For this reason it was decided to measure the pressure distribution at a number of stations along the wetted side of the hydrofoil as well as at several places along the tunnel wall.

As the flow configurati n in question is restricted to the fully cavitating and the fully separated (bu without cavity formation) condition, the suction side is covered entirely by a flow region of nearly constant pressure. A single tap was found adequate enough to measure the cavity pressure or the wake under-pressure.

There are several advantages in making the pressure measurements. In the first place no tare forces and moments on the model support need be calibrated and the effect due to the small gap between the model and tunnel windows can be neglected as the pressure tap holes are located far from these gaps. A further advantage was noted at the preliminary stage of data reduction; it was found that the pressure coefficients are more sensitive to the tunnel wall effect than the forces and the moments. This finding has led to a practical method of estimating the necessary correction for the wall effect.

In order to facilitate a large number of models to be tested in this experimental program as well as future studies of the optimum profile, a basic model support was designed and constructed for this general purpose. It serves as the common main body to which a hydrofoil of different profile and flap deflection can be easily fastened, or interchanged, for testing. This model support can be permanently mounted to span across the tunnel, with its cylindrical base passing through a hole in the tunnel wall. The ducts and tubes imbedded in this model support, as shown in Figure 1, serve as passages leading from the pressure holes in the model face to the pressure tubes outside the tunnel.

The complete model as shown in Figure 2, consists of the main body of six inch span and the removable parts, whose outer surface bears the required hydrofoil profile and whose inner surface was made entirely flush at the interface with the main body. The pressure holes drilled across these removable parts lead directly to the passages in the main body; the sealing of the pressure leads at the intersection was accomplished with O-rings, seated in the main body (Figure 1 at right).

The basic profile has a simple wedge outline with a vertex angle of 9 degrees and a length of the pressure side $c = 6$ inches which is also the chord length of the hydrofoil. The vertex angle of 9 degrees was chosen

for the material stiffness, though it limited the smallest incidence for the lifting flow to about 5 degrees. In the present program the removable parts have the simple configuration of flat plates, each covering 0.2 of the chord, except for the leading segment which has a length of 0.4 chord. This part tapers towards the leading edge.

Different configurations of the flap were achieved by replacing one or more of the rear plates by wedge shaped prisms whose pressure side has basically the same length as its base so that the flap length, denoted by f, remains fixed at different flap deflections. The wedge angle of the prisms gives the desired flap angle $\epsilon\pi$ (see Figures 3, 4).

For measuring the pressure distribution along the pressure side, a row of 1/32 inch pressure holes were drilled along the center of the 6 inch span of the removable parts at a distance of 1/30 chord apart and with two additional holes at 1/60 chord length from the leading and trailing edges (Figure 5). Furthermore additional pressure taps were installed at the intersection of each consecutive pair of removable parts. This was done in order to measure the pressure at the hingepoints and to find if the local pressure deviates from the stagnation pressure ($\frac{1}{2}\rho V^2$) as predicted by the inviscid flow theory. To prevent leakage through the interface, the two opposing surfaces were greased before they were mounted together.

Because of the small tapering of the forward part of the model, the pressure holes in this part could not just be drilled through the plate. Instead, tubes were laid in the plate, leading to a row of holes, distributed spanwise in the main body, slightly to the rear of the leading edge. The method of using the sealed breaks in the pressure leads proved to be fully satisfactory.

As only the fully cavitating and fully separated flows were dealt with, the back side of the main body was kept simple. Figure 1 shows the open recess and layout of the brass tubings and the openings for air supply (for forced ventilation when necessary) and for measuring the cavity pressure or the base under-pressure in the separated wake flow. This measurement of cavity pressure was performed by measuring the static pressure near the discharge end in a 3/16 inch wide tube, through which slow moving water was directed, keeping the probe wet. The discharge of water into the recess

from a relatively wide tube was supposed to eliminate interference from capillarity. By using this system, the cavity pressure could be treated in exactly the same way as all the other pressures.

Facility and Experimental Set-up

The experiments were performed in the High Speed Water Tunnel of the California Institute of Technology, using the new two-dimensional working section (6). This tunnel is equipped with a three component balance for stationary flows to which the hydrofoil model was fastened.

For the measurement of pressure distribution, a 6 feet high, 21 tube multimanometer, filled with mercury and water was used. The reference pressure was taken from a point upstream of the nozzle (total head of the flow). Two tubes in the multimanometer were used for measuring the average static pressure in the working section, upstream of the model, and the cavity pressure (or the wake under-pressure). Readings of the multimanometer were recorded by a modified "Recordak" camera. The side profile of the hydrofoil model and the cavity were recorded simultaneously with the data reading of each run by a second "Recordak" camera. An example of this pair of recordings is shown in Figure 6. Separate measurements of the velocity head and tunnel static pressure were also made with separate mercury manometers for the convenience of conducting the experiment.

The average static pressure upstream of the hydrofoil was taken from a manifold connected through resistors with 15 taps distributed along the height of the working section, approximately one chord upstream of the leading edge of the hydrofoil.

Experimental Procedure

Prior to each run the angle of attack of the model was set at a specified value. The manometer tubes were checked for air bubbles and bled if necessary. Values of the pertinent flap-chord ratio, flap angle, angle of attack and other specifications of the run were indicated on the multimanometer. Each set of runs was started at a static pressure, measured by the separate manometer, or approximately 10 psi gage and was generally followed by measurements at 5 and 0 psi gage. The velocity was set to

give a maximum manometer reading of 1.5 feet for p_k, or somewhat less in case the flow showed noticeable unsteadiness; the latter measure was taken to provide an adequate safety margin for the model and its support. All the photographic records, automatically numbered, were then taken after the mercury column heights had reached a sufficiently constant state.

For the succeeding measurements, air was supplied to the suction side of the model and the pressure level in the tunnel lowered to give different values of the cavitation number. After a total of approximately nine runs with gradually decreasing cavitation number, the pressure control became deficient due to the generation of a large air pocket in the tunnel diffuser. This difficulty could be overcome to an extent by releasing water from the tunnel into an evacuated vessel at the same time when air was supplied to the model suction side. The deficiency of further pressure control marked the end of each set of runs. Reynolds numbers between 0.6×10^6 and 1.5×10^6 were obtained during the runs.

Tunnel Wall Effect

The wall correction for experiments with thin bodies in windtunnels is fairly well established (7). For the cavitating flow past a model in a water tunnel however, the situation is further complicated by the presence of a free boundary as well as a solid boundary and by the fact that the body-cavity system is often not thin compared with the channel width. In the simple case of choked cavity flow (with the cavity extremely long in a water tunnel) past a flat plate set normal to the stream, it has been shown by Birkhoff, Plesset and Simmons (8) that the wall correction for the drag coefficient C_D is small if it is based on the velocity at the cavity boundary, but may be very large if based on the upstream velocity. However, for the more general case of lifting flows with a finite cavity, no definite formula or rules have been established for correcting the wall effect. In this series of experiments, it has been found that the local pressure coefficient is more sensitive to the wall effect than the force coefficients and therefore a reliable wall correction is necessary to present a meaningful result. Fortunately an empirical rule has been established here for wall correction, which is supported by observations with geometrically similar models of three differ-

ent sizes.

The first series of experiments was conducted with pressure measurements from 18 holes along the wetted side of the model, together with the measurement from the cavity pressure tap and the manifold for the tunnel static pressure. The choice of the stations along the pressure side was such that in the regions of large pressure gradient, successive stations were used; these regions include those near the leading edge, trailing edge, and in and on both sides of the hingepoint. In the two remaining regions, some pressure holes were skipped and not used.

After the first set of data was reduced on the basis of the measured upstream velocity and static pressure, the resulting C_p values (which will be referred to in this report as C_{p_o}) compare rather poorly with the theory. The discrepancy between C_{p_o} and the theoretical prediction is however in a consistent trend, with a rather uniform difference, as shown in Figure 7. In this comparison no correction was made for the tunnel wall effect.

In an earlier experiment Parkin (9) was able to obtain some good agreement for the force coefficients with nearly the same theory (Wu 1955) without making any such corrections. As the ratio of the model chord to the tunnel height (c/T) in the present case was only little larger than in Parkin's experiments, it could be expected that again the wall effect should be small. But now poor agreement between the C_p values necessitates an investigation of the wall effect. On the other hand, integration of the pressure over the body surface showed that the pressure coefficients are more sensitive to the wall effect than the force and moment coefficients. This can easily be understood, if one considers that C_p is a function of the position along the chord where it is measured and so is the error of C_p. At the leading and trailing edges of the model and in the forward stagnation point the error is zero as a consequence of the method of data reduction used. If it is assumed that the cavity pressure is used as reference pressure, it is clear that the force coefficient is equal to the average of the pressure coefficients and likewise is the error of the force coefficient equal to the average of the errors of the pressure coefficients, which must be less than the maximum error of the pressure coefficients. This maximum error is definitive for the comparison. If a different pressure than the cavity pressure is used for reference pres-

sure, it can be easily shown that the difference between the pertinent errors is increased with increased σ.

Although the value of σ should reduce to zero as the cavity becomes very long, it is well known that in a tunnel this is never reached if velocity and pressure are related to the working section pressure in undisturbed flow. At a certain critical $\sigma_c > 0$, the cavitation index can not be reduced further; this is known as "choking" or "blockage" of the tunnel. Contrary to what is suggested by these terms, it is still possible to increase the average tunnel velocity, but σ remains unchanged because of a simultaneous increase of the average tunnel static pressure. From experience and theory (Cohen (10)) it is known that the larger the ratio c/T, the higher σ_c is. This phenomenon, which is the most important influence of the presence of the tunnel walls on cavitation flows, is what in this report is referred to as "wall effect".

In cases when an extremely long cavity was recorded, an attempt was made to improve the correlation in data reduction by expressing the pressure coefficient based on the pressure and velocity adjacent to the cavity. To this end p_o and V_o were corrected theoretically by using Bernoulli's equation and the over-all continuity condition. The latter depending on the working section cross sectional area reduced by the cross sectional area of the cavity at the downstream end of the tunnel window, which was measured from the photographic recording. The result of this attempt gave a nearly perfect correlation between experiment and theory with the value of σ equal to zero. This type of wall correction in which both σ and C_p were corrected is in agreement with Birkhoff, Plesset and Simmons (8). In the case of the infinite cavity within tunnel walls it is known that the flow far downstream is parallel and constant. The pressure at the cavity boundary therefore must be equal to that in the main stream according to the present method of wall correction and hence it corresponds to the case $\sigma = 0$ in an unbounded flow.

Such a simple consideration for long cavities must however be modified for the general case of moderate and short cavity lengths.

At this point, with all the model configurations already tested, it was decided to make use of the versatility of the model and have new flaps made which could be combined with the available face plates to form half size and three quarter size hydrofoil models in order to find a practical

solution to the wall correction problem. The combinations of the model parts are sketched in Figure 4. It should be noted that only those flow conditions would be valid where the rear part of the main body would be fully enveloped by a wake or cavity.

Some consideration was given to the measurement of the minimum pressure on the upper or lower tunnel wall; it appears that this pressure can represent the static pressure in infinite flow better than any other pressure available in the tunnel. This minimum pressure at the tunnel wall should occur adjacent to the cavity if the viscous effect is neglected and it should occur at a point where the streamlines are horizontal. The pressure gradient in the flow direction at this point is zero and the transverse gradient can be shown to be zero on account of the small curvature of the streamlines near this point.

For this reason pressure taps were made in the lower window of the working section, which were connected to the multimanometer, thus reducing the number of recording stations on the model to 9. With this set-up measurements were made, starting with the smallest model size and the data were reduced on the basis of the minimum pressure (not necessarily the lowest) on the tunnel bottom.

Figure 8 gives an example of the results. It shows that with this method a very reasonable agreement is obtained between the experimental C_p values (here referred to as C_{pm}) for the models of different sizes and the theoretical results (11). As a comparison Figure 7 shows another set of data which are now reduced on the basis of the upstream average pressure p_o, again without other corrections. It is shown that the minimum value of σ_o depends on the model size and on the flow conditions. Furthermore it is found that the relationship between C_{p_o} and σ_o for very large cavity length can be expressed by the formula of a straight line which intersects the $\sigma = 0$ point of the theoretical curve and the point (-1, 1); hence

$$(1 - C_p)/(1 + \sigma) = \text{const.} \qquad (1)$$

The constant is determined by the condition that C_p assumes the theoretical value at $\sigma = 0$. This means that the points related to the choked flow condition obtained experimentally with models of different sizes can be made to coincide with the theoretical result of the infinitely long cavity by

shifting the experimental points along the line of Eq. (1). This shift of experimental data can be achieved effectively by taking the minimum pressure p_m on the wall to replace p_o and the flow velocity at the same point to be the reference velocity in the definition of C_p and σ. The results of this rule for wall correction is so effective that the dependence of model scale is seen to be practically eliminated.

With the measurement of pressures along the tunnel bottom included, the tests were repeated with all model configurations, in order to obtain a full set of data as a result of the method based on the minimum bottom pressures under various conditions. The example of Figure 6 was taken from these tests.

In order to be able to use the original data obtained with 18 stations along the pressure side of the model, an adequate method had to be found for reducing those data. The relationship between σ_{in} and σ_o could not be used since the variation of the required value σ_m is very large compared with the variation of the available quantity based on the upstream average pressure p_o. The only reasonable method seemed to be to estimate the minimum bottom pressures (p_m) by comparing the length of the cavities from the photographic recordings in comparable flow conditions (Figure 9). Due to dynamic effects in the flow and the presence of much air in the wake behind the cavities, the estimate was not precise, but was nevertheless adequate.

To show the relationship between the upstream average pressure and σ_m, C_{pm} values for the upstream cross section of the tunnel are plotted in Figure 10, in which the scale effect can also be noticed. In the Figures 11 and 12 an example is given of plots of tunnel bottom pressure coefficients, to show the influence of σ_m and model size respectively.

Data Reduction

The data* obtained from the multimanometer and the cavity lengths, both by photographic recording, were used for reduction (Figure 6). The heights of the mercury columns (h) were read in feet and immediately corrected for parallax (-0.002 through +0.001 feet). As the pressure upstream of the nozzle was taken as reference pressure for the multimanometer, all the column heights gave the measure of the pressure

* The tabulated data are available upon request.

difference between the total head and the local pressure:

$$\gamma h = H - p.$$

It can be shown that the local pressure coefficient, based on any reference quantity (index r) can be easily derived from a simple division of column heights:

$$1 - C_p = h/h_r. \tag{2}$$

In the various data plots, the values of $1 - C_p$ were simply plotted downwards from the value $C_p = 1$.

With $h_r = h_{pm}$, the column height for the pressure at the point of minimum wall pressure, equation (2) reduces to:

$$1 - C_{pm} = h/h_{pm}.$$

The cavitation number σ_m was obtained in the same way, considering that $\sigma_m = -C_{pm}$ for the back of the model:

$$1 + \sigma_m = h_{pk}/h_{pm}.$$

To reduce the amount of work, h_{pm} was approximated by the minimum value obtained at the stations instead of using a faired minimum. No significant error was introduced by this approximation.

Correlation with Theory; Errors

Theoretically and experimentally obtained pressure coefficients for several stations have been compared as a function of the cavitation number. This has been done for all configurations of the model, with almost the same results in all cases. An example is shown in Figure 13. The agreement is reasonable to very good.

In judging the discrepancies which do occur, the following possible experimental errors should be taken into account:

1. The multimanometer zero level may have been approximately 0.002 feet low, which is due to a lack of rigidity of the floor and the thickness of the zero line on the manometer scale. The exact level was not clearly discernable and the error was therefore neglected.
2. The meniscus of the mercury columns reflected the light in such a way that it was difficult to perceive precisely. Readings may have

been 0.003 feet low for this reason.

3. The mercury columns in the multimanometer were inter-connected by a manifold, which in turn was connected to the well. This system gave rise to swinging of the mercury with a tendency for the high columns on one side to be over-estimated and the low columns on the other side to be under-estimated. This means that model face pressure readings may have been up to 0.035 feet low (in few extreme cases - 0.035 feet was read near the stagnation point); tunnel bottom pressure readings may have been the same amount high (which led to $1 + \sigma_m < 1$).

The extreme total error is estimated at 0.040 feet low reading for the model and 0.035 feet high reading for the minimum pressure at the tunnel bottom and p_k. This leads to experimental C_p values which may have been 0.071 high (for instance in one case when $\epsilon\pi = 0^\circ$, $\alpha = 69.85^\circ$, $\sigma_m = 0.305$, at station 29 which is near to the trailing edge). Those extreme errors occurred with the larger α values as a result of dynamic effects in the flow.

Discrepancies were found, ranging from -0.090 through +0.105, if the region near the hingepoint is neglected. The extreme negative deviation occurred only in regions with a very large pressure gradient and at very low σ values, when vapour lock in the manometer leads may have caused a large error. Some low points were plotted for the smallest α values at higher cavitation numbers. These should be neglected as it is doubtful that full separation occurred in these cases.

When the possible errors are taken into account, it must be concluded that the probability is large that the theory is correct in all cases considered, except for the region near the hingepoint

Hingepoint Separation

At the hingepoint of the flap the experimental C_{pm} values were found to deviate considerably from the theoretical value, which in this case is one.

In Figure 14, a selection of theoretical and experimental pressure distribution curves are compared. The theoretical curves have been calcu-

lated for a cavitation number value for which experimental data were available, obtained with 18 pressure holes. Other data, obtained under comparable conditions with nearly equal σ were added if they were available. The curves show that just upstream of the hingepoints a large positive pressure gradient is predicted by the theory. It is well known that the boundary layer at a body is not capable of resisting such a rise in pressure and therefore separation of the flow should be expected. The occurrence of this is confirmed by the experiments. In Figure 15 complete plots are given of all the pressure coefficients obtained in the hingepoints, including those obtained with the smaller scale model configurations.

Corrections for Theoretical Forces and Moments

Of major interest to most designers of hydrofoils are the forces and moments which can be anticipated in the various conditions. To obtain these directly from the experiments is illogical, as the integration of the experimental pressure data can not be achieved by the same accuracy as can be obtained from the theory. For that reason no force and moment coefficients are given here. A comprehensive set of curves of lift coefficients, leading edge moment coefficients, hinge-moment coefficients and lift-drag ratios, can be found in a separate paper by Harrison and Wang (11).

In order to be able to account for the influence of hingepoint separation, corrections were estimated from average experimental pressure coefficients in this region. The results are given in Figure 16. The corrections should always be subtracted from the theoretical values. Because the viscous effect is small, the corrections were estimated only for the worst conditions, which are defined by a small cavitation number and a small angle of incidence. Low σ values mean low C_p values and consequently low values for the force and moment coefficients and a large rise towards the theoretical stagnation pressure. A low cavitation number is connected with wide peaks and therefore a wide separated region.

As a basis for the estimate it was considered that at the point of separation and at the point of re-attachment of the flow, discontinuities in the pressure curves may exist and that probably the region of separation can be treated as a constant pressure region as is done in a wake.

A rather coarse approximation could be allowed, for the related error would be of the second order small, with the correction itself being only up to 3% of the force and moment coefficients. The approximation consists of the replacement of the theoretical C_p distribution curves on both sides of the hingepoints, by straight lines. In this way the integration of the triangle between the theoretical and experimental C_p distributions will probably be somewhat over-estimated, which may be counterbalanced by the fact that the experimental C_p values will probably be a little on the high side, as has been discussed before.

Cavity Lengths

As has been discussed earlier, the cavity length data have been used as a basis for the achievement of values of the minimum pressure at the bottom of the working section, in those cases when no direct measurement of this quantity was performed. All these cases were related to the largest model scale. In one case also the cavity lengths have been measured for the half size model configuration. The plotting of both sets of data in one diagram (Figure 17) has disclosed the interesting fact that the length of long cavities is much influenced by the proximity of the tunnel walls. It was found that in comparable conditions the smaller model has the longer cavity relative to its chord length. Although no direct comparison is possible, this finding seems to be in accordance with the results obtained theoretically by Hirsh Cohen and DiPrima (10) for a 15° wedge in symmetrical flow.

Dynamic Effects

At all the angles of attack, but more so at larger angles, dynamic effects could be observed in the flow. It seems possible that these effects have the same cause as the Kármán vortex street behind a cylinder for instance. It must be noted however that a rather elastic support has been used, which was the force balance, and which caused severe oscillations of the angle of attack to occur in extreme cases.

Conclusions

From the results of the present experiments it can be concluded

that the free streamline theory by Wu gives extremely good results for fully separated wake and full cavity flows around flapped flat plate hydrofoils. The theory fails in a small region near the hingepoint of the flap, where the sharp rise of the pressure causes separation of the flow. The influence of this separation on the generated forces and moments is very small and can be neglected at larger angles of attack. With small α values and small flap length ratios however, the influence runs into several percents.

It was found that the tunnel wall effect can not be neglected with full cavity flow experiments. Measurements with different scale models and theory were found to be in good agreement with each other, if the unbounded flow conditions at infinity were supposed to exist in a point at the pressure side tunnel wall where the pressure had its minimum value.

Acknowledgment

The author is indebted to those working in the Hydrodynamics Laboratory of the California Institute of Technology for their assistance, co-operation and interest in his work during his academic visit in Pasadena, while on leave of absence from the Technical University of Delft. He is also indebted to the Technical University of Delft and The Netherlands Organization for Pure Research "Z. W. O." for the support of his visit at the California Institute of Technology.

REFERENCES

1. Birkhoff, G. & Zarantonello, E. H., 1957, "Jets, Wakes and Cavities." New York, Academic Press Inc.

2. Gilbarg, D., 1960, "Jets and Cavities." Handbuch der Physik, Vol. 9, 311-445. Berlin, Springer Verlag.

3. Wu, T. Y., 1962, "AWake Model for Free Streamline Flow Theory Part I: Fully and partially developed wake flows past an oblique flat plate." J. Fluid Mech., Vol. 13, 161-181.

4. Wu, T. Y. & Wang, D. P., 1964, "A Wake Model for Free Streamline Theory, Part II: Cavity flows past obstacles of arbitrary profile." J. Fluid Mech., Vol. 18, 65-93.

5. Fage, A. & Johansen, F. C., 1927, "On the Flow of Air Behind an Inclined Flat Plate of Infinite Span." Proc. Roy. Soc., Vol. 116, 170-197.

6. Kiceniuk, T., 1964, "A Two-dimensional Working Section for the High Speed Water Tunnel at the California Institute of Technology." ASME; Cav. Res. Fac. and Tech.

7. Pope, A. "Wind-Tunnel Testing." John Wiley & Sons Inc., N. Y., Chapman & Hall Ltd., London.

8. Birkhoff, G., Plesset, M. & Simmon, N., 1950, "Wall Effects in Cavity Flow." 1, Quar. Appl. Math. 8, 151-168; II, ibid. 9 (1952), 413-421.

9. Parkin, B. R., 1956, "Experiments on Circular Arc and Flat Plate Hydrofoils in Noncavitating and Full Cavity Flows." J. S. R., Vol. 1, 4, 1958, 34-56.

10. Cohen, Hirsh & Diprima, R. C., 1958, "Wall Effects in Cavitating Flows." Sec. Symp. on Nav. Hydro. (O. N. R.)

11. Harrison, Z. & Wa[illegible]. P., 1965, "Evaluation of Pressure Distribution on a C[illegible]ng Hydrofoil with Flap." California Institute of Techno[illegible]port No. E-133.1.

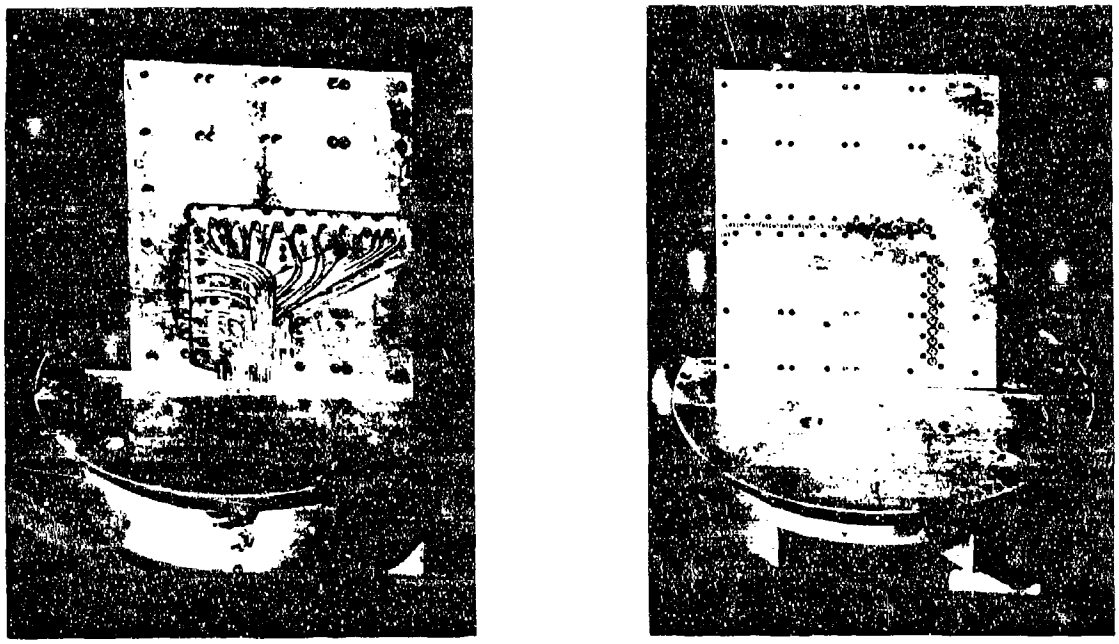

Fig. 1. Suction side (left) and interface side (right) of the hydrofoil main body.

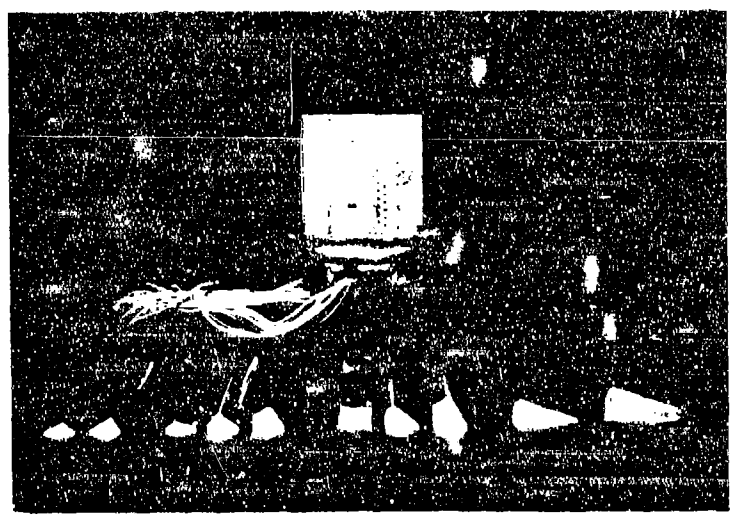

Fig. 2. Mounted hydrofoil model with complete set of flaps. The pressure sides are all facing to the right.

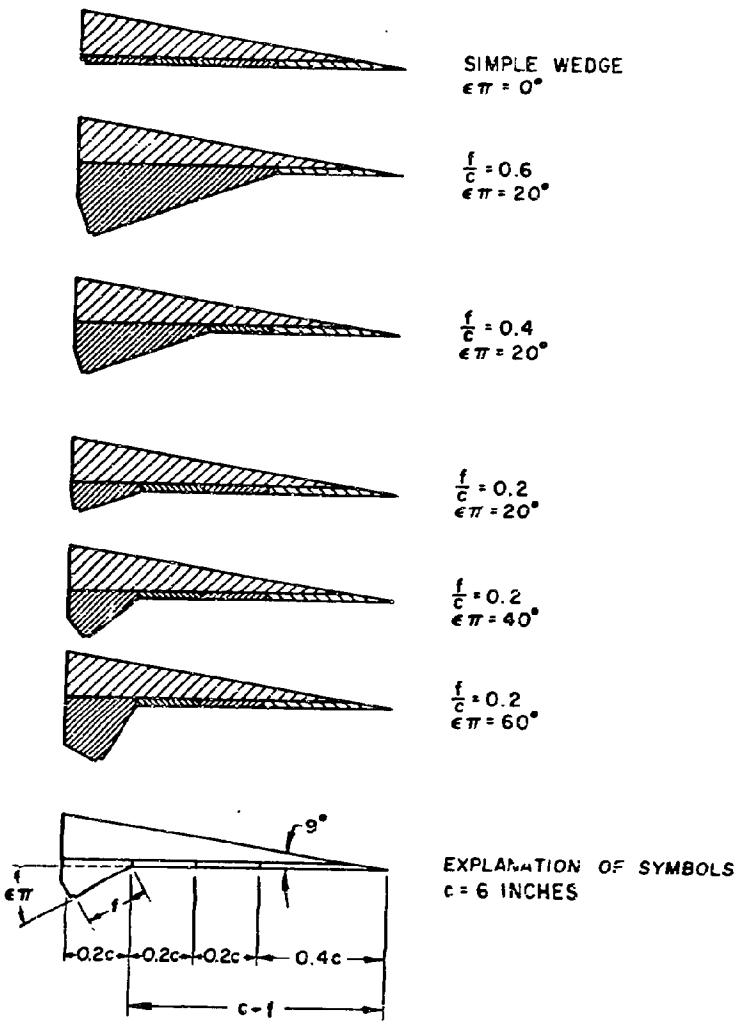

Fig. 3. Original model configuration profiles.

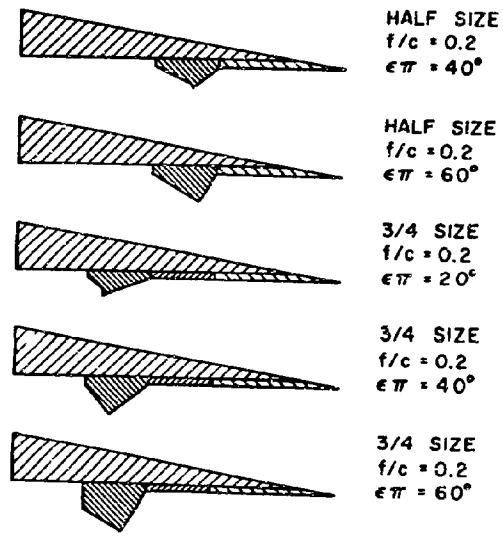

Fig. 4. Additional scale model configuration profiles.

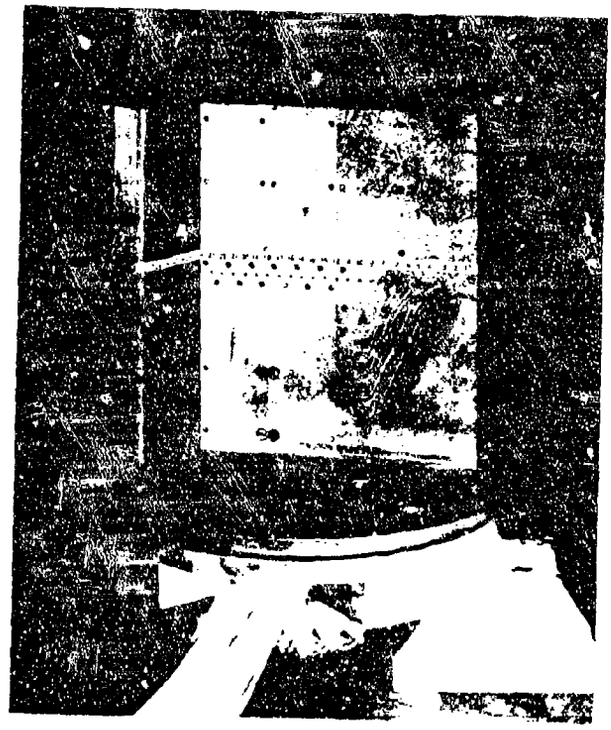

Fig. 5. Fully mounted hydrofoil model with flap, seen from the pressure side. The pressure openings are numbered as shown.

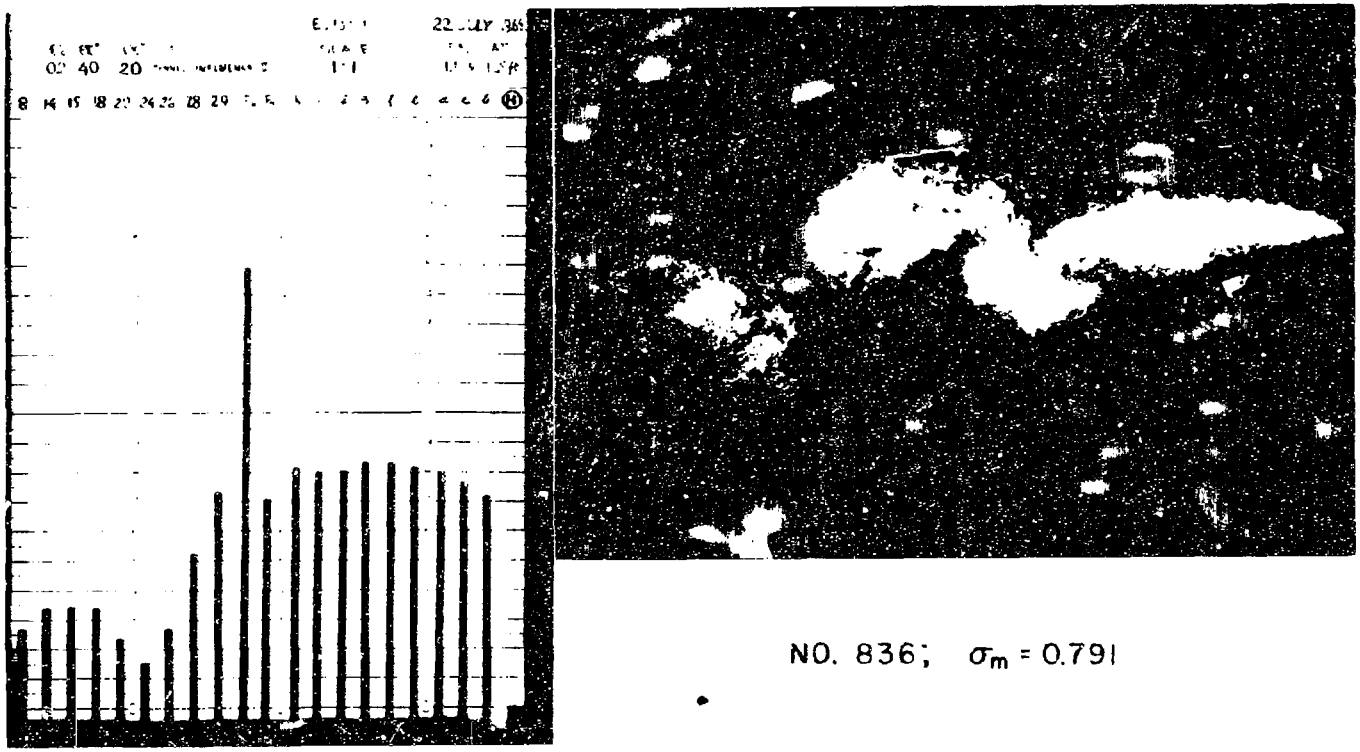

Fig. 6. Example of a pair of photographic recordings.

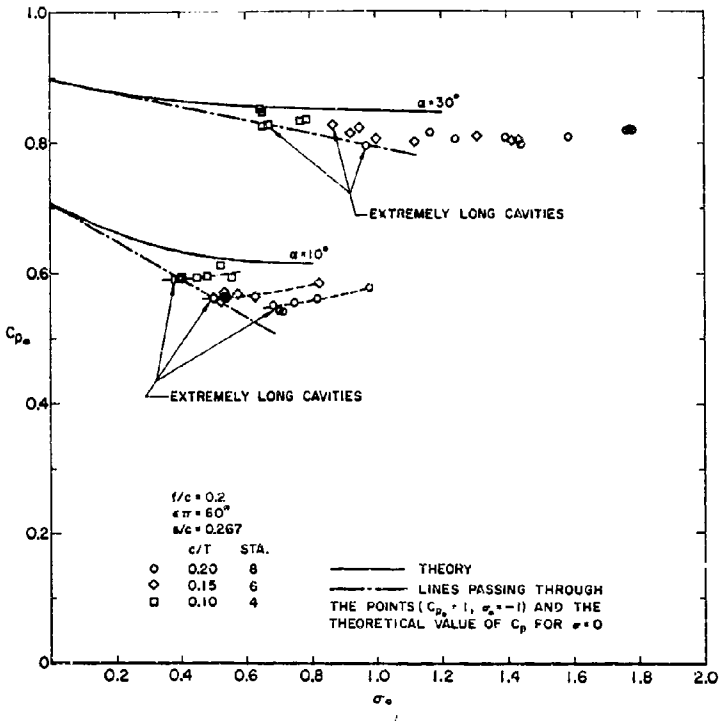

Fig. 7. The influence of the size on the pressure coefficient when σ and C_p are based on the upstream average pressure.

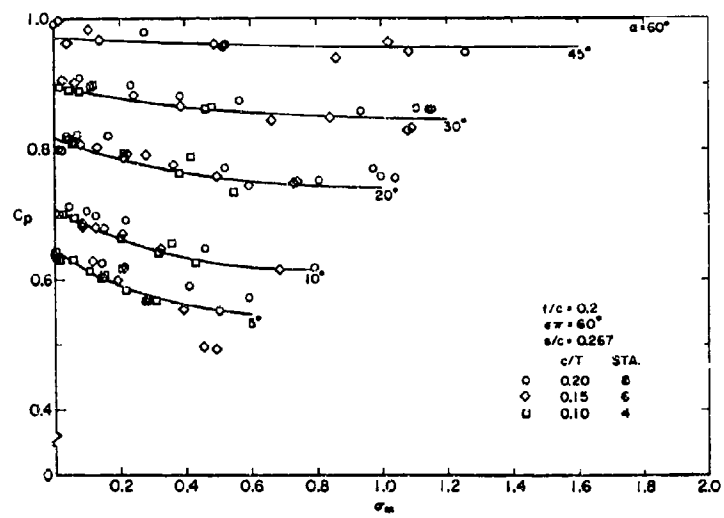

Fig. 8. Comparison of pressure coefficients, obtained for the same relative station with three model sizes and from theory. σ and C_p were based on the measured minimum pressures at the tunnel bottom.

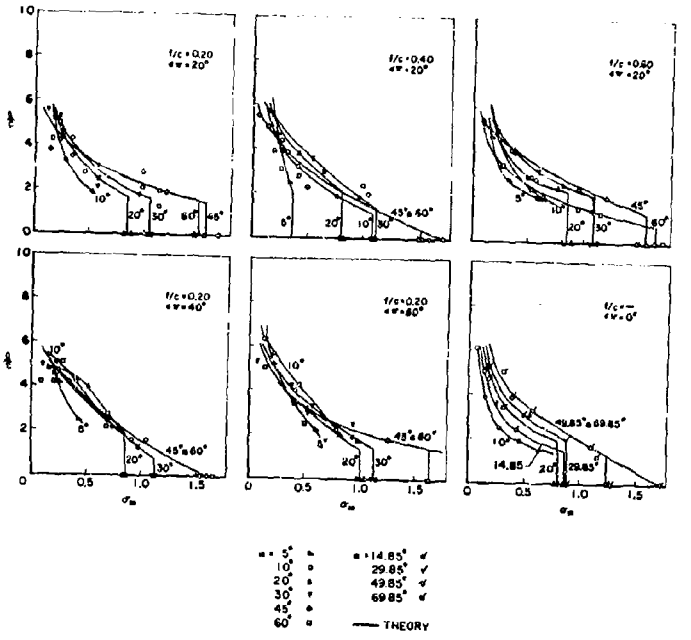

Fig. 9. Curves of cavity length ratios, used for the estimate of σ_m in those cases, where no readings of wall pressures were available.

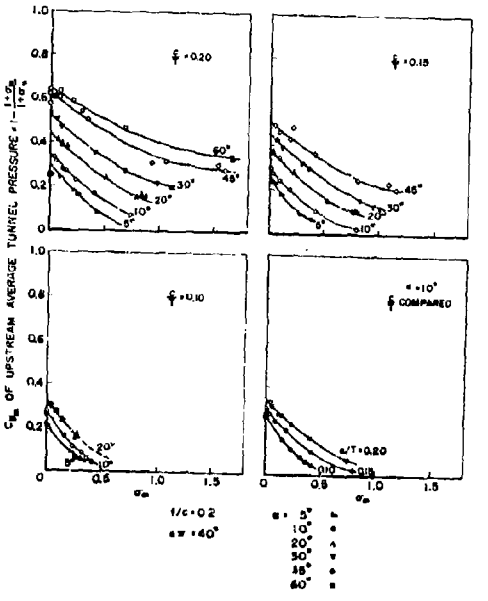

Fig. 10. Influence of model size on the upstream average pressure coefficient, based on the minimum pressure at the tunnel bottom.

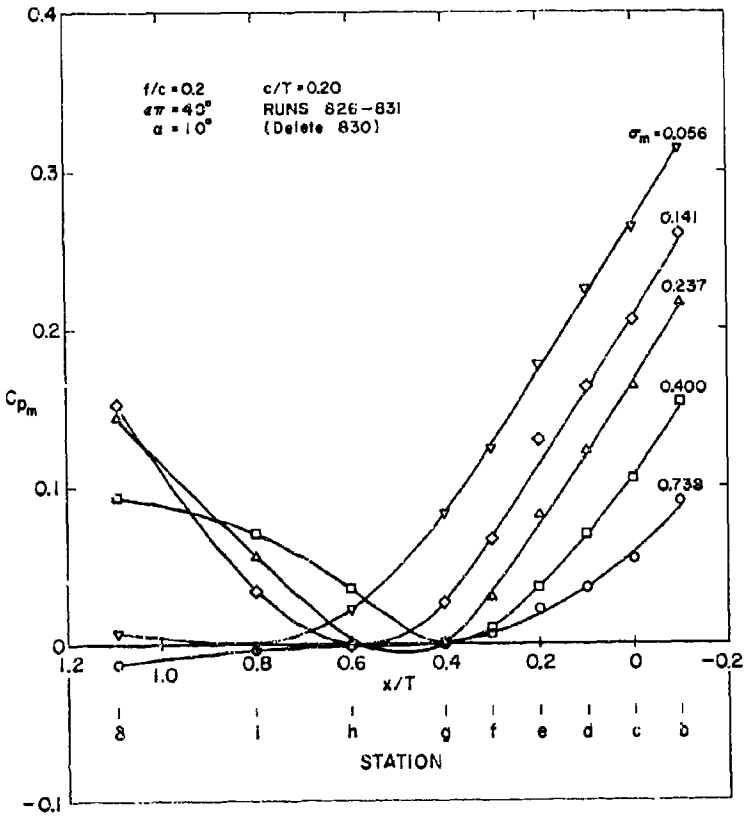

Fig. 11. The influence of σ_m on the pressure distribution along the tunnel bottom.

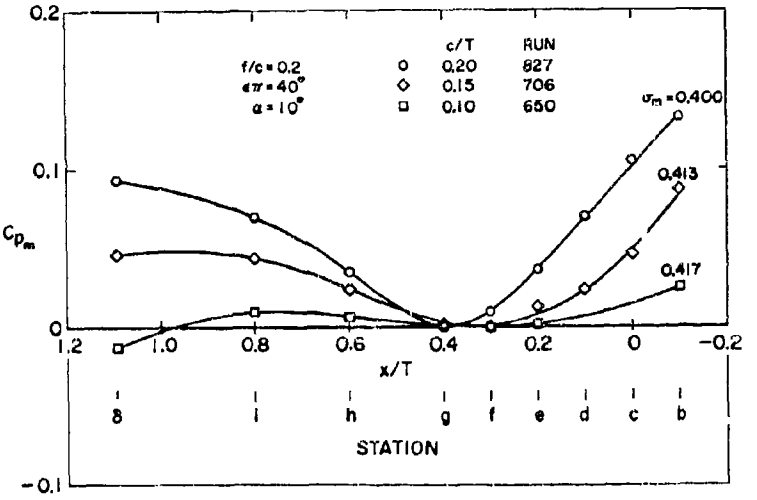

Fig. 12. The influence of model size on the pressure distribution along the tunnel bottom.

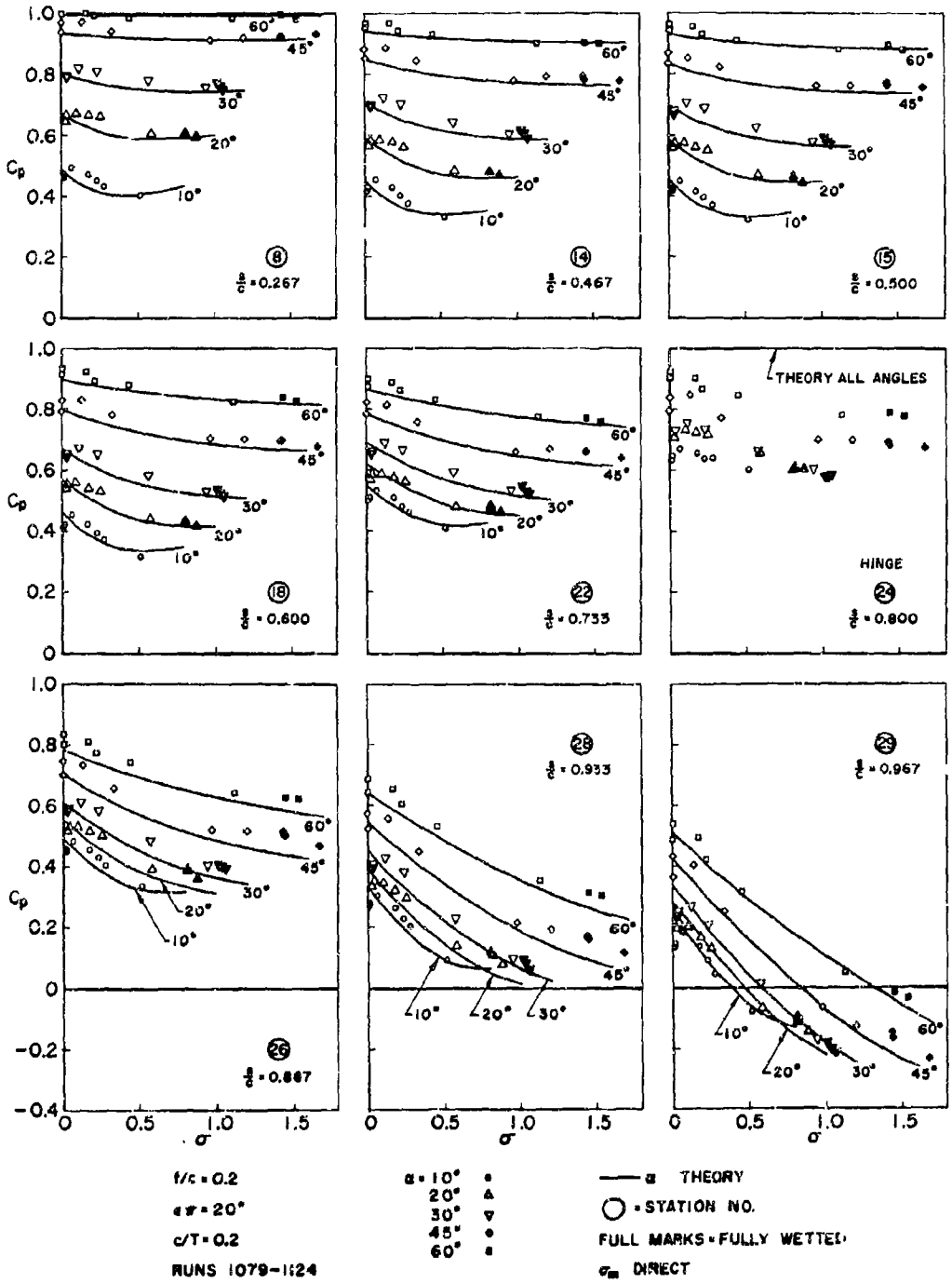

Fig. 13. Correlation example.

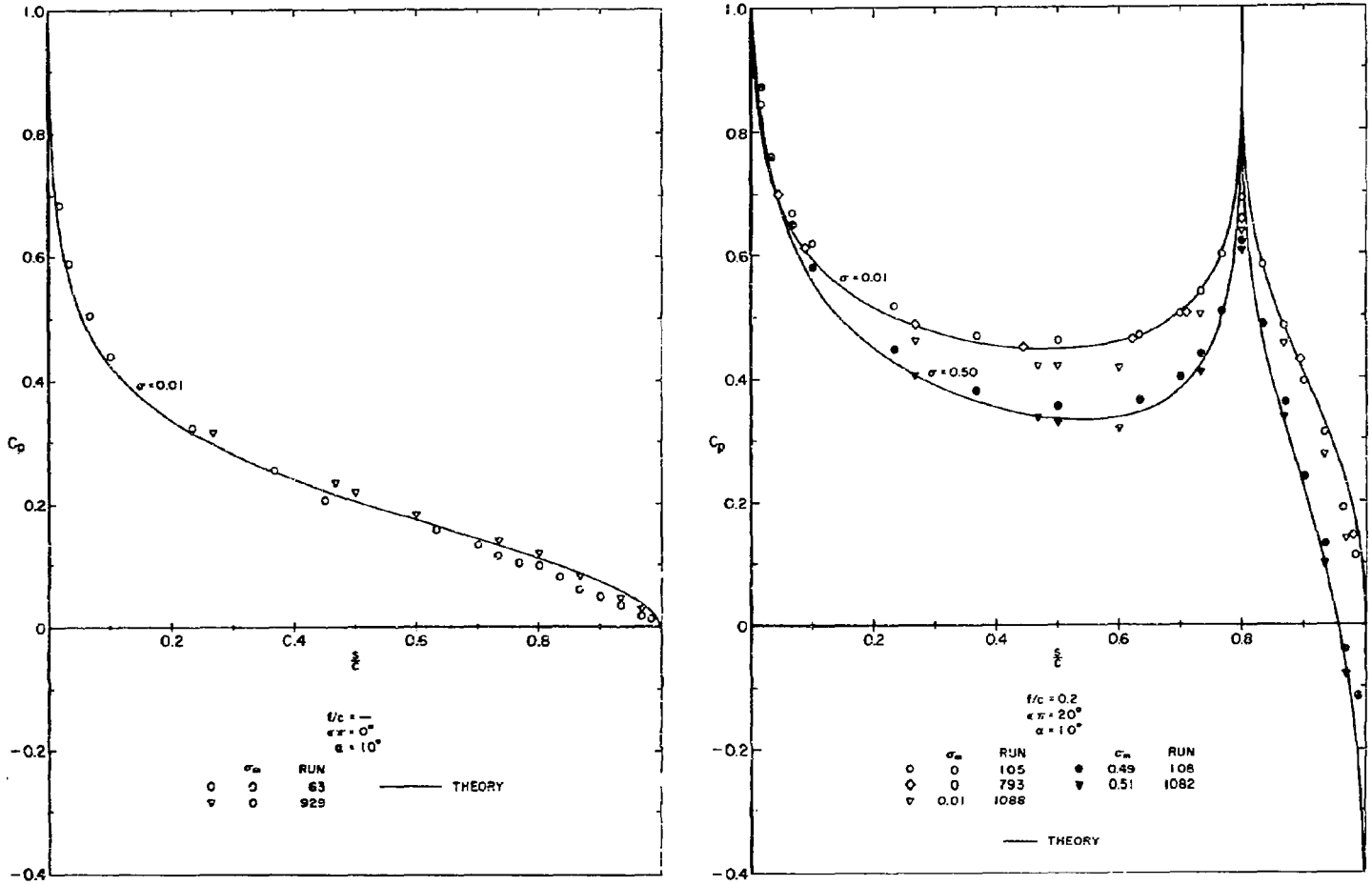

Fig. 14-1 and Fig. 14-2. Examples of pressure distribution correlations.

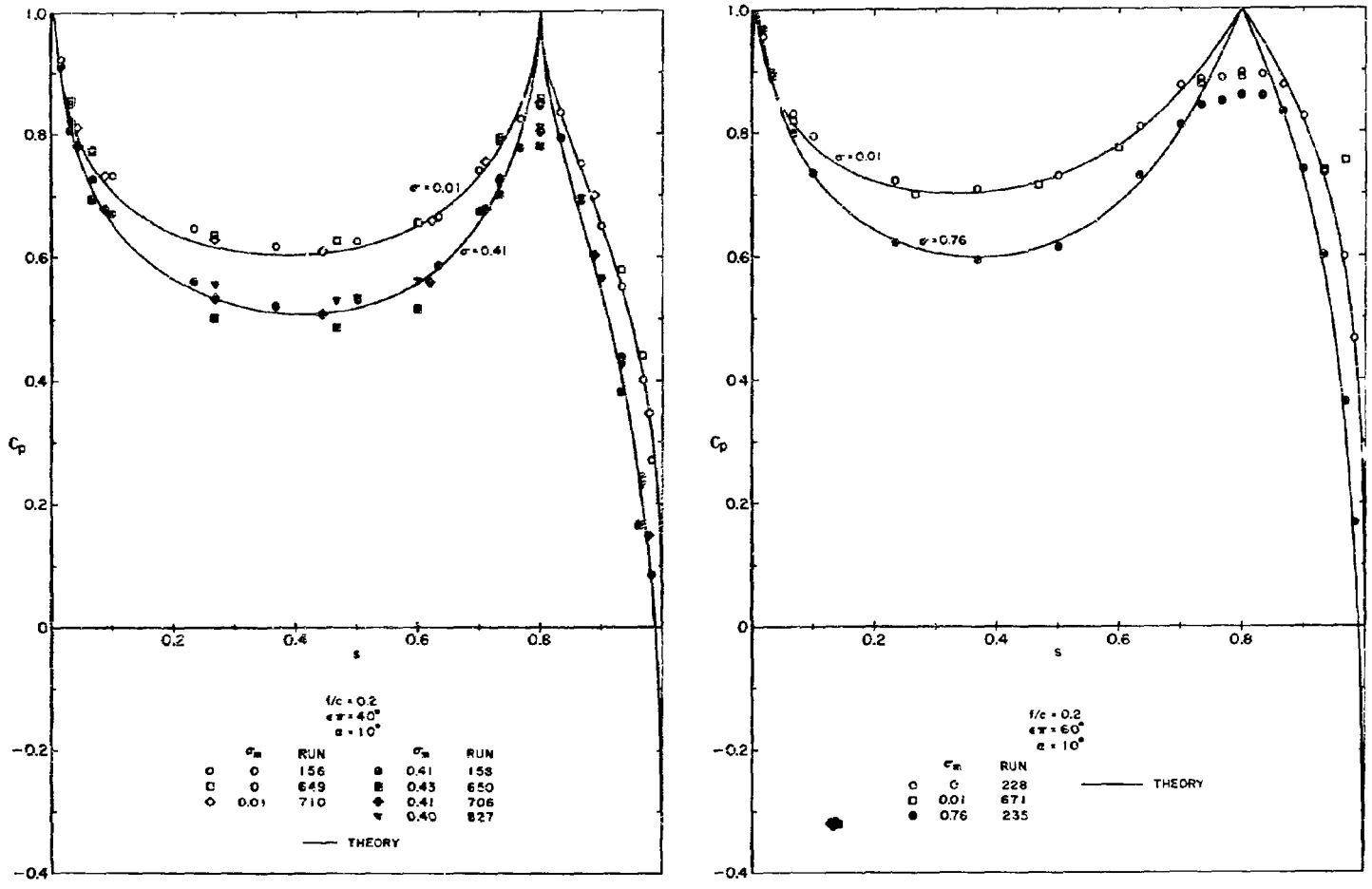

Fig. 14-3 and Fig. 14-4. Examples of pressure distribution correlations.

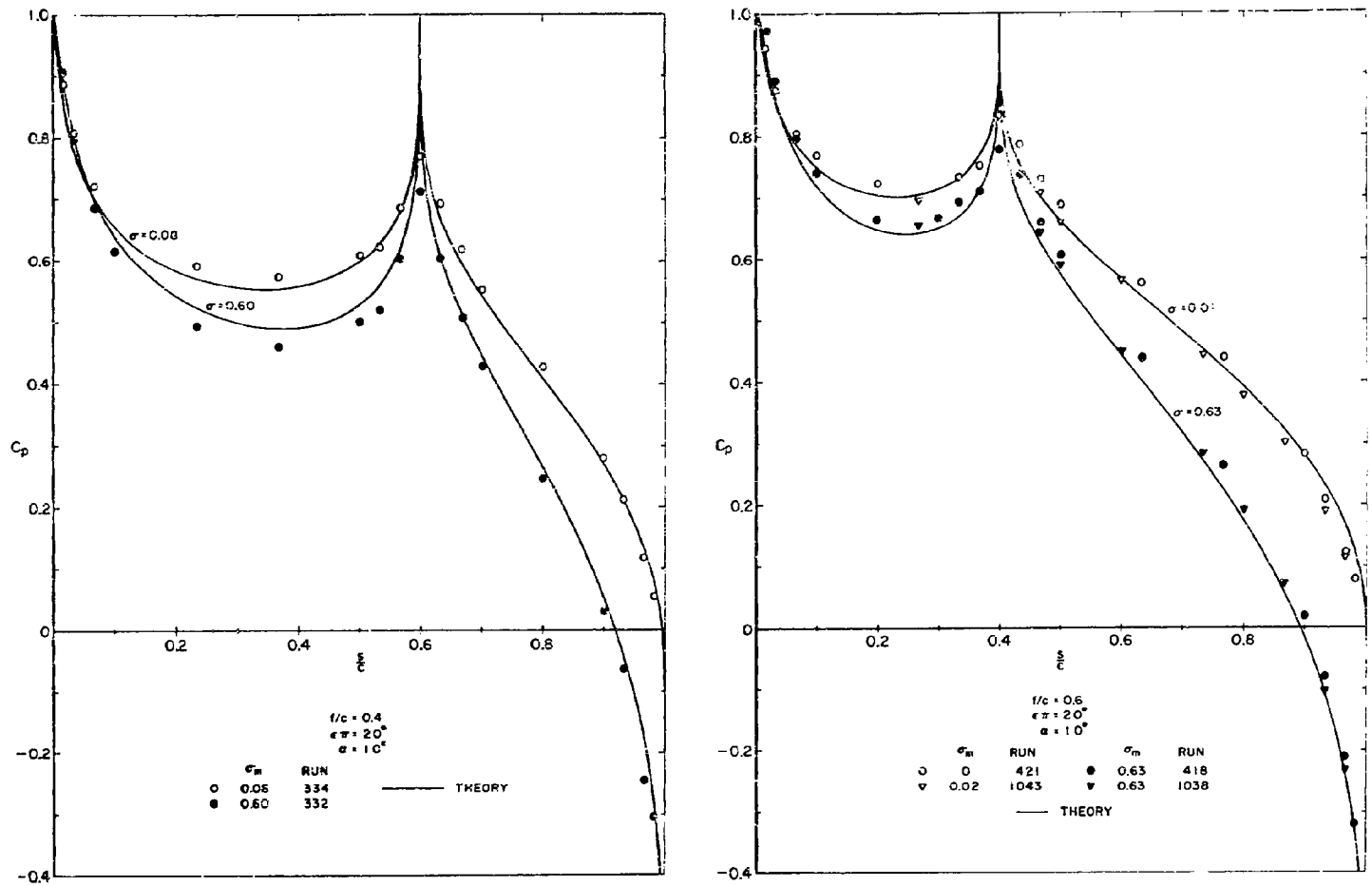

Fig. 14-5 and Fig. 14-6. Examples of pressure distribution correlations.

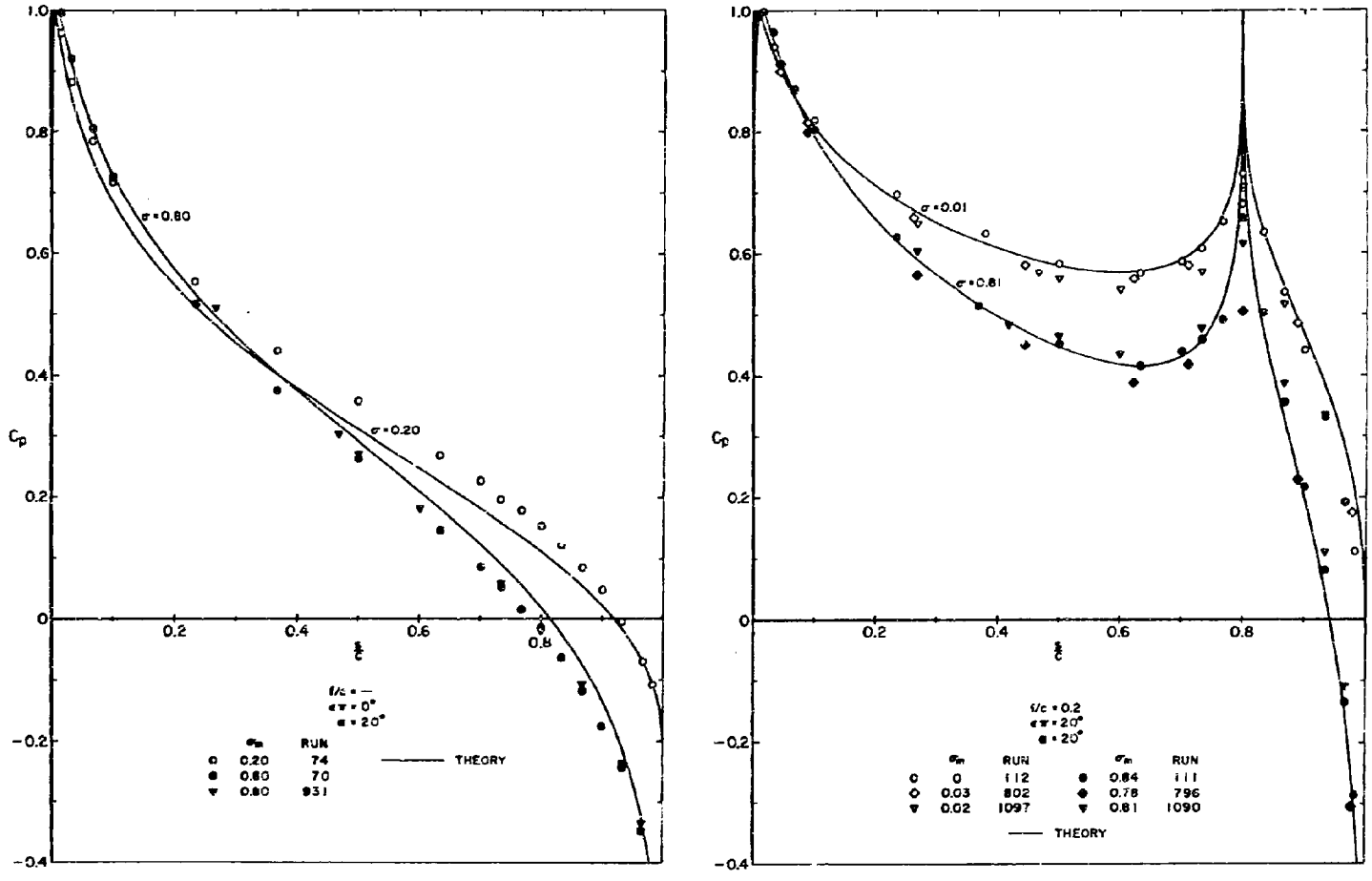

Fig. 14-7 and Fig. 14-8. Examples of pressure distribution correlations.

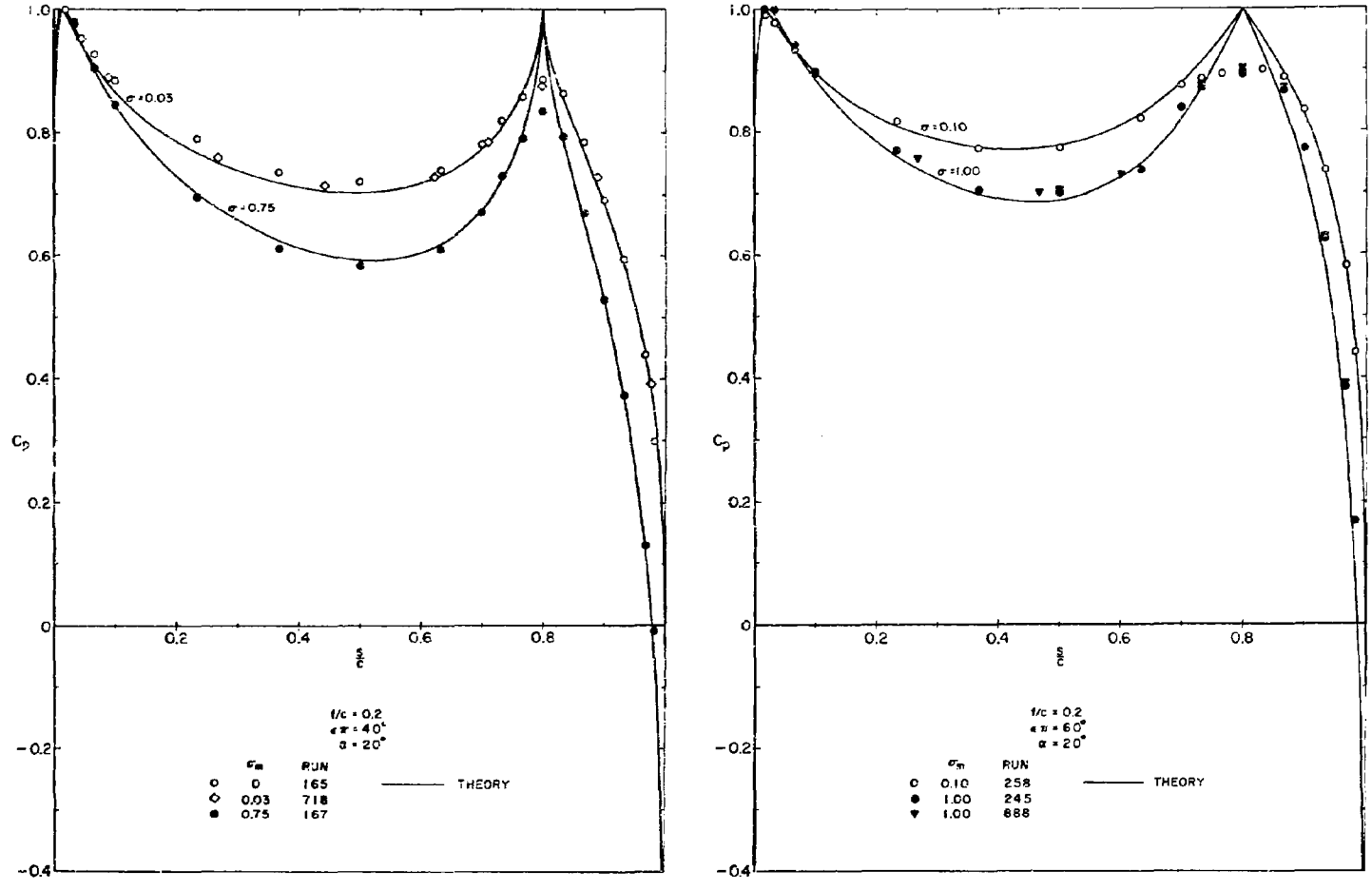

Fig. 14-9 and Fig. 14-10. Examples of pressure distribution correlations.

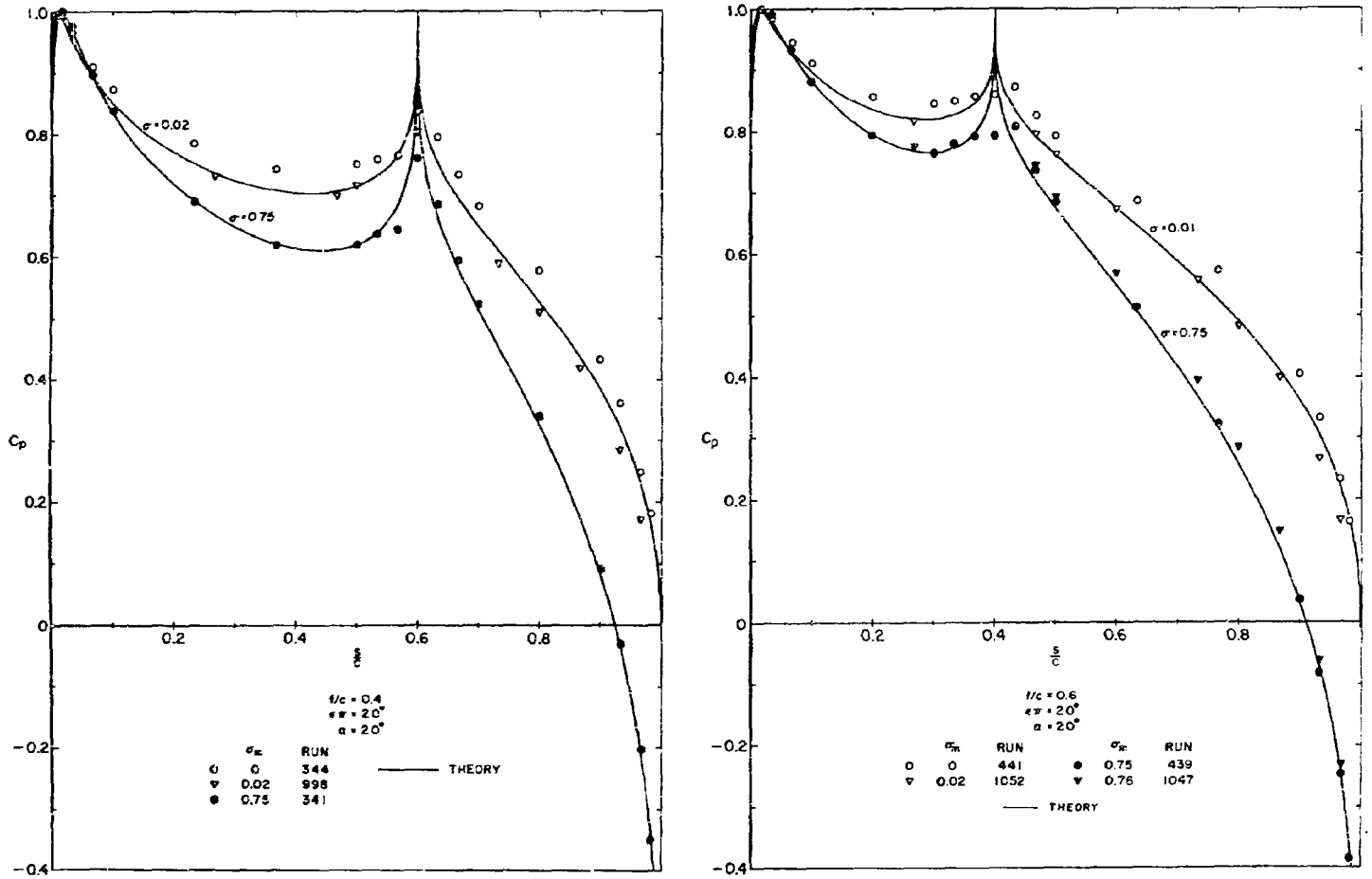

Fig. 14-11 and Fig. 14-12. Examples of pressure distribution correlations.

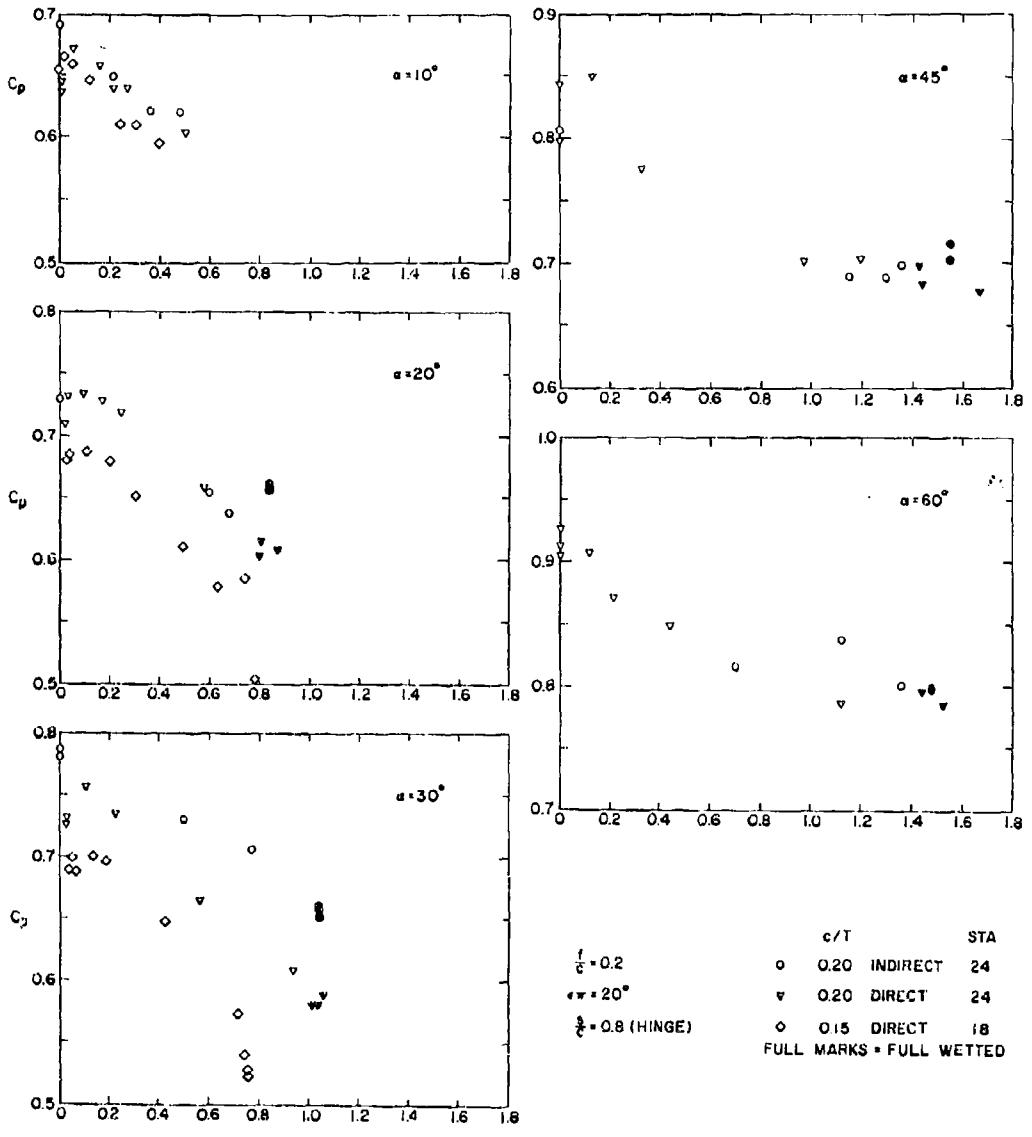

Fig. 15-1. Hingepoint pressure coefficients.

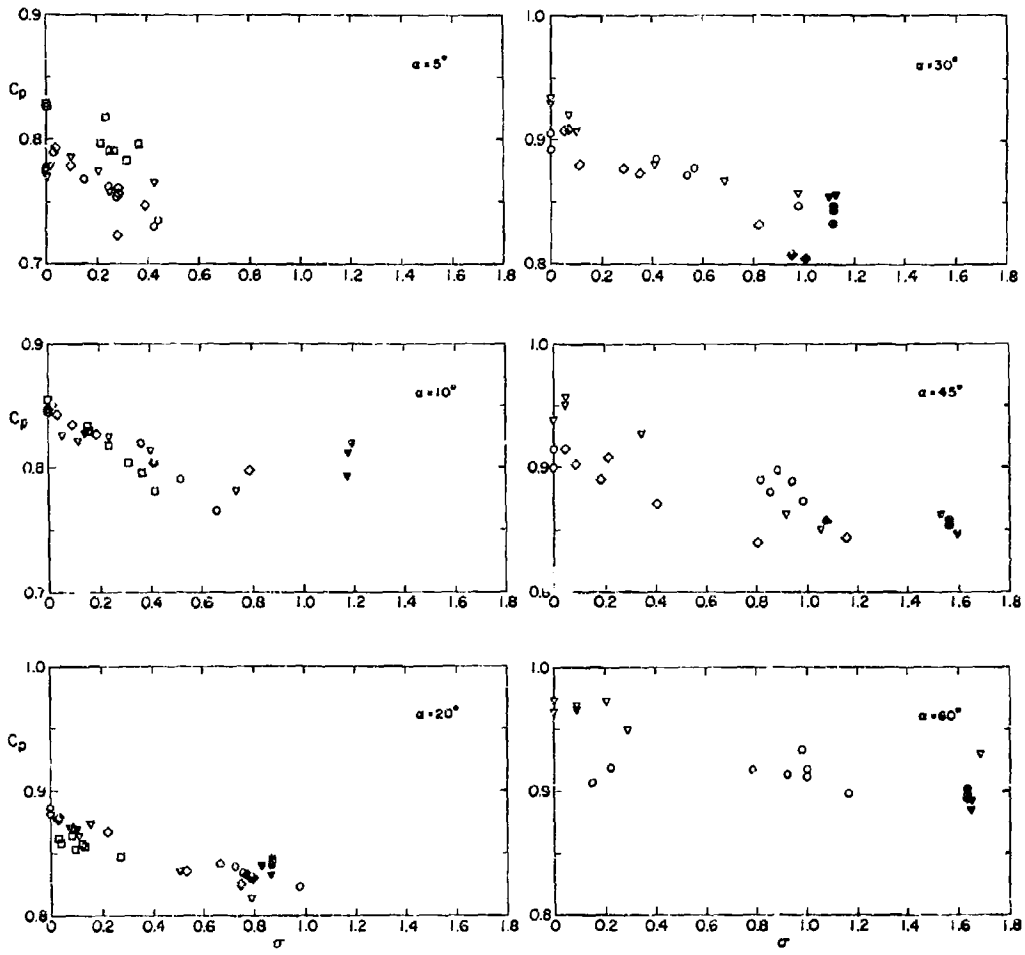

$\frac{t}{c}$ = 0.2
α_v = 40°
$\frac{x}{c}$ = 0.8 (HINGE)

	c/T		STA
○	0.20	INDIRECT	24
▽	0.20	DIRECT	24
◇	0.15	DIRECT	18
□	0.10	DIRECT	12

FULL MARKS = FULL WETTED

Fig. 15-2. Hingepoint pressure coefficients.

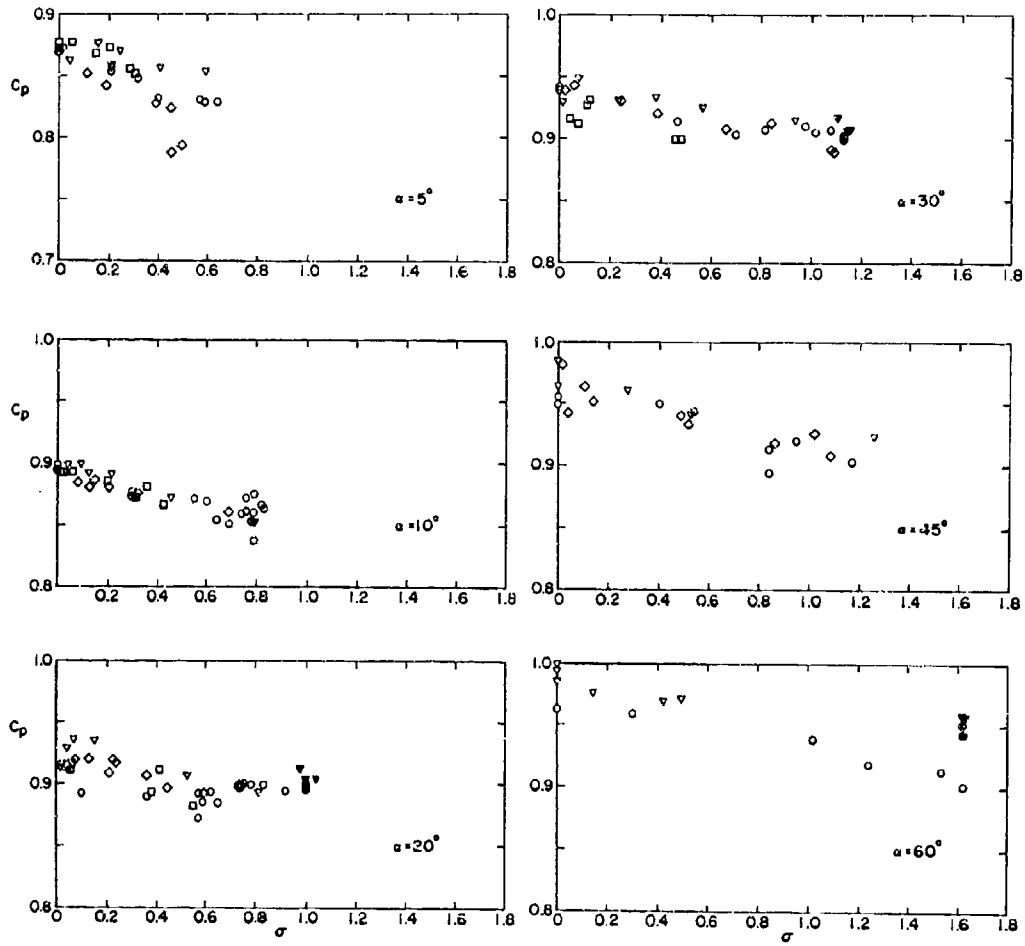

	c/T		STA
$\frac{f}{c}$ = 0.2	○ 0.20	INDIRECT	24
α = 60°	▽ 0.20	DIRECT	24
$\frac{s}{c}$ = 0.8 (HINGE)	◇ 0.15	DIRECT	18
	□ 0.10	DIRECT	12

FULL MARKS = FULL WETTED

Fig. 15-3. Hingepoint pressure coefficients.

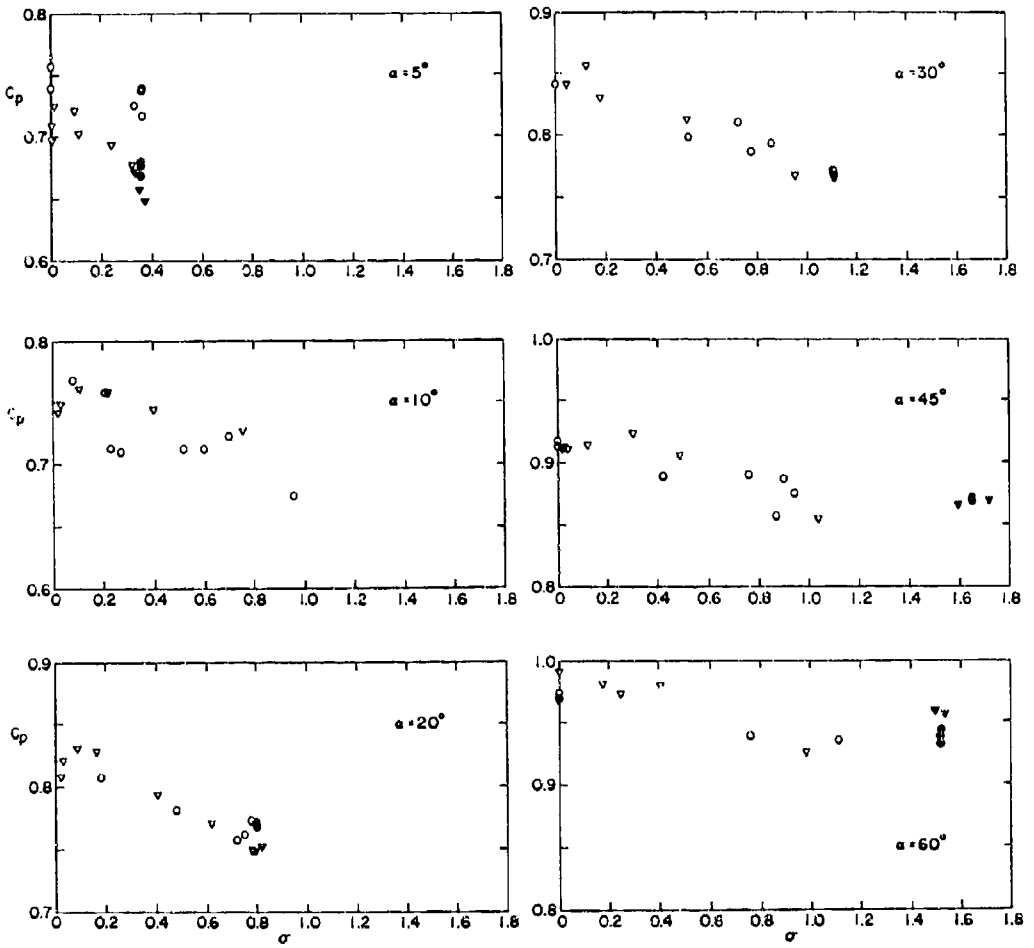

Fig. 15-4. Hingepoint pressure coefficients.

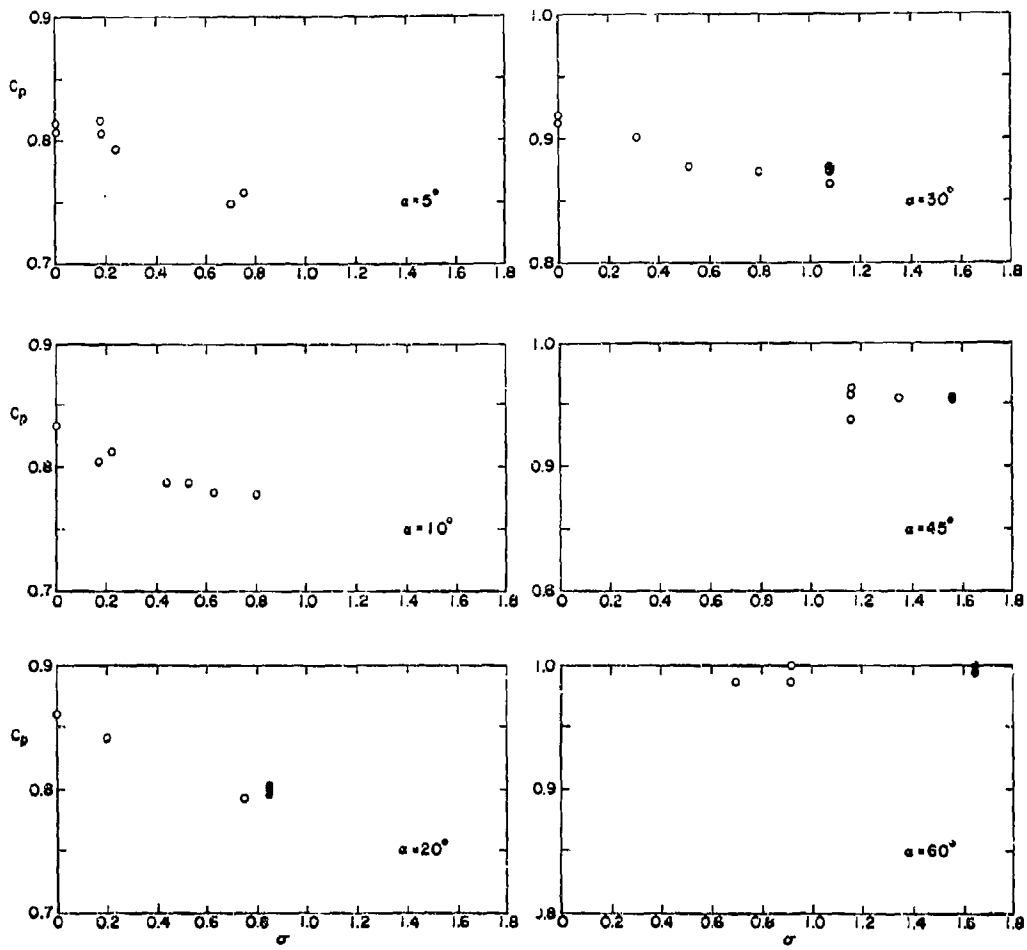

Fig. 15-5. Hingepoint pressure coefficients.

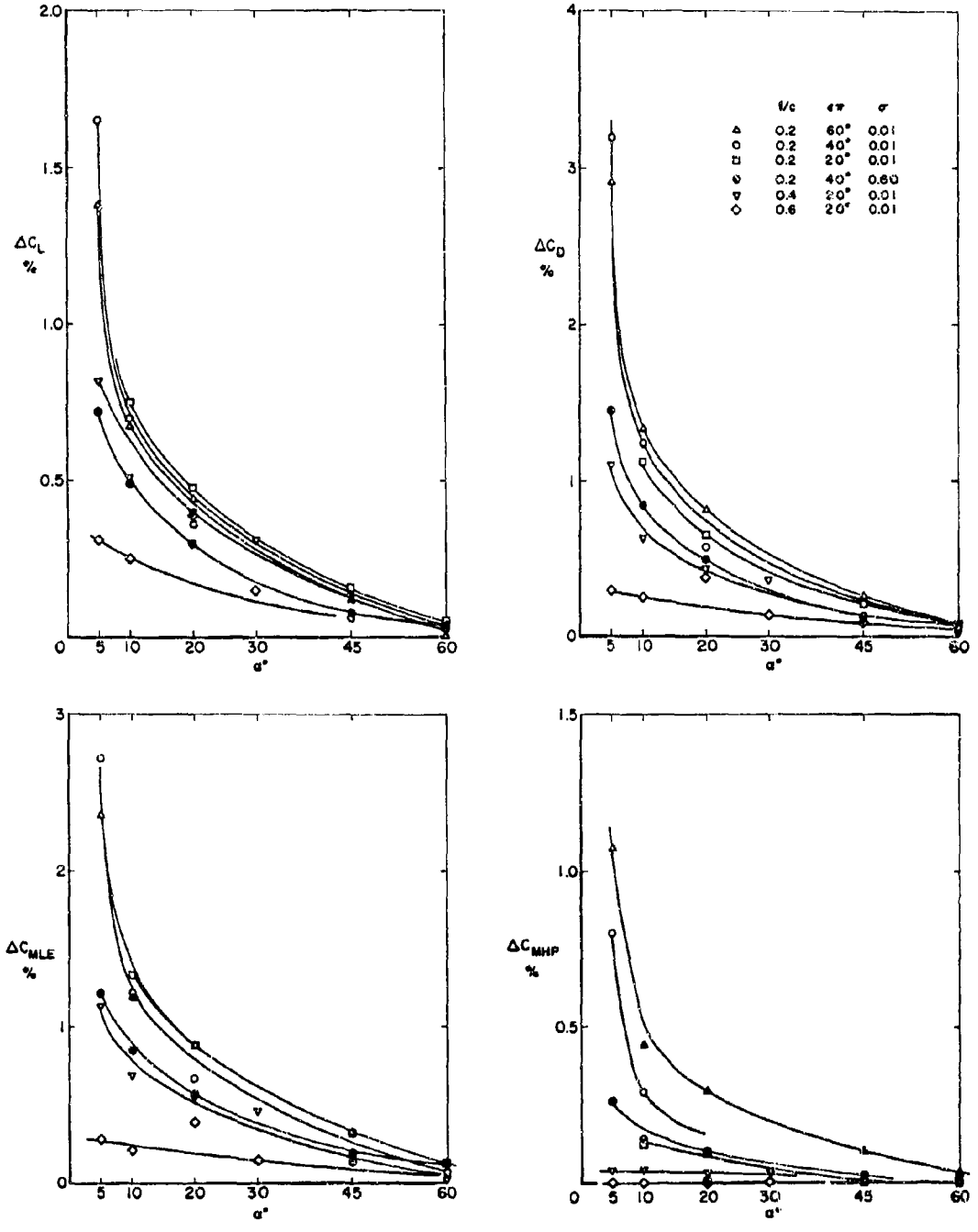

Fig. 16. Hingepoint separation corrections for force and moment coefficients.

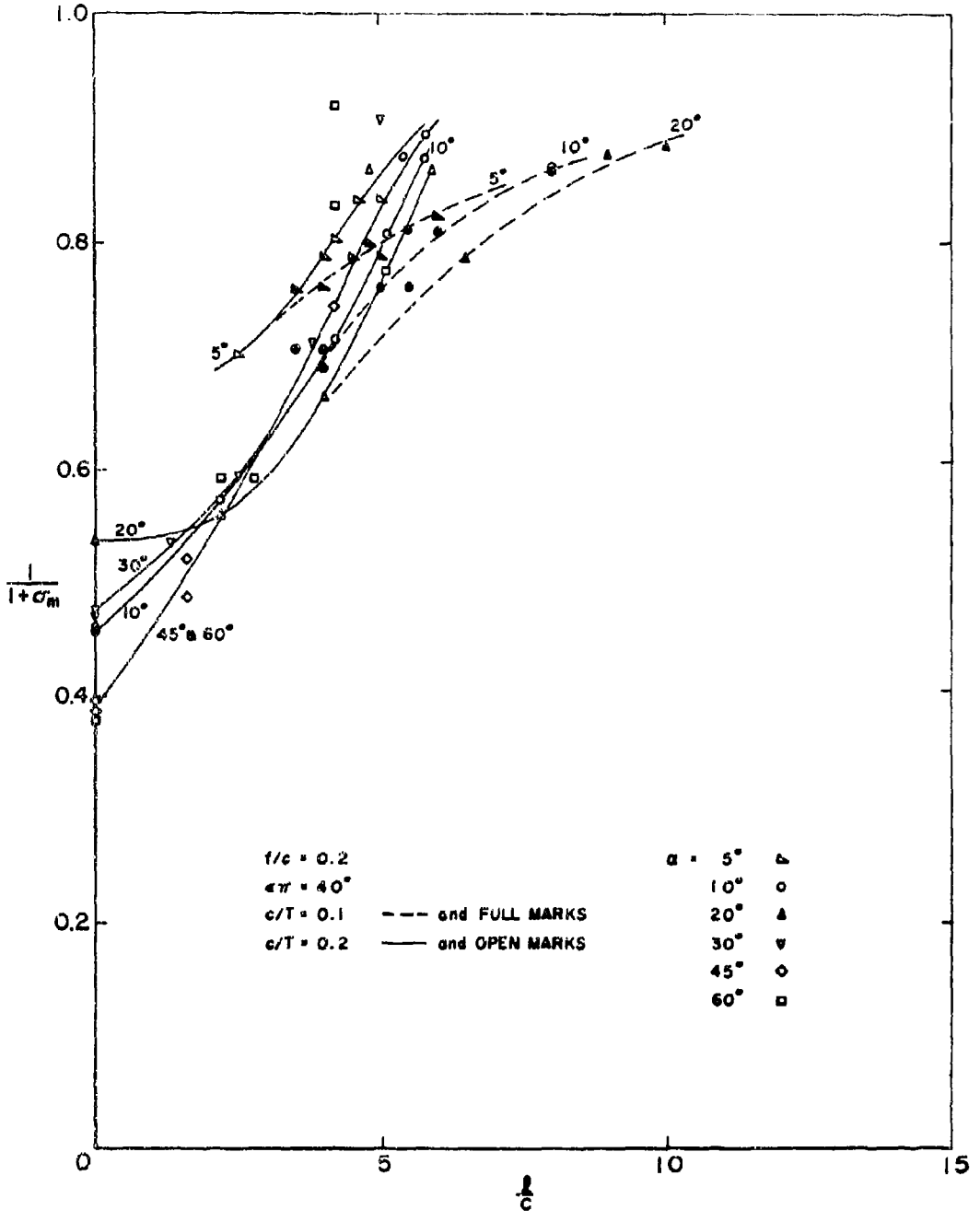

Fig. 17. Wall effect on cavity length.

Unclassified

Security Classification

DOCUMENT CONTROL DATA - R&D

(Security classification of title, body of abstract and indexing annotation must be entered when the overall report is classified)

1. ORIGINATING ACTIVITY (Corporate author)	2a. REPORT SECURITY CLASSIFICATION
California Institute of Technology	Unclassified
	2b. GROUP

3. REPORT TITLE

Pressure Measurement on Flapped Hydrofoils in Cavity Flows and Wake Flows

4. DESCRIPTIVE NOTES (Type of report and inclusive dates)

Final

5. AUTHOR(S) (Last name, first name, initial)

Meijer, M. C.

6. REPORT DATE	7a. TOTAL NO. OF PAGES	7b. NO. OF REFS
October 1965	37	11

8a. CONTRACT OR GRANT NO.	9a. ORIGINATOR'S REPORT NUMBER(S)
Nonr-220(52)	
b. PROJECT NO.	E-133.2
c.	9b. OTHER REPORT NO(S) (Any other numbers that may be assigned this report)
d.	

10. AVAILABILITY/LIMITATION NOTICES

"Qualified requesters may obtain copies of this report from DDC."

11. SUPPLEMENTARY NOTES	12. SPONSORING MILITARY ACTIVITY
	Dept. of the Navy Office of Naval Research

13. ABSTRACT

The purpose of the present experiments is to obtain a detailed information about the flow field, such as the pressure distribution, at the surface of a flapped hydrofoil in full cavity or wake flows. The model and the experimental procedure are described. The experimental results obtained have been used to compare with the theoretical predictions, to investigate the tunnel wall effect and to estimate the viscous effect at a sharp corner. An empirical method for correcting the tunnel wall effect is developed here, the validity of which is supported by tests with models of three different sizes. An appreciable viscous effect has been found near the hinge of a deflected flap. Except for this effect, the theory and experiments are found to be in good agreement.

DD FORM 1 JAN 64 1473 0101-807-6800

Unclassified

Security Classification

14. KEY WORDS	LINK A		LINK B		LINK C	
	ROLE	WT	ROLE	WT	ROLE	WT
1. Wake Flows 2. Flapped Hydrofoils 3. Pressure Measurement						

INSTRUCTIONS

1. ORIGINATING ACTIVITY: Enter the name and address of the contractor, subcontractor, grantee, Department of Defense activity or other organization *(corporate author)* issuing the report.

2a. REPORT SECURITY CLASSIFICATION: Enter the overall security classification of the report. Indicate whether "Restricted Data" is included. Marking is to be in accordance with appropriate security regulations.

2b. GROUP: Automatic downgrading is specified in DoD Directive 5200.10 and Armed Forces Industrial Manual. Enter the group number. Also, when applicable, show that optional markings have been used for Group 3 and Group 4 as authorized.

3. REPORT TITLE: Enter the complete report title in all capital letters. Titles in all cases should be unclassified. If a meaningful title cannot be selected without classification, show title classification in all capitals in parenthesis immediately following the title.

4. DESCRIPTIVE NOTES: If appropriate, enter the type of report, e.g., interim, progress, summary, annual, or final. Give the inclusive dates when a specific reporting period is covered.

5. AUTHOR(S): Enter the name(s) of author(s) as shown on or in the report. Enter last name, first name, middle initial. If military, show rank and branch of service. The name of the principal author is an absolute minimum requirement.

6. REPORT DATE: Enter the date of the report as day, month, year; or month, year. If more than one date appears on the report, use date of publication.

7a. TOTAL NUMBER OF PAGES: The total page count should follow normal pagination procedures, i.e., enter the number of pages containing information.

7b. NUMBER OF REFERENCES: Enter the total number of references cited in the report.

8a. CONTRACT OR GRANT NUMBER: If appropriate, enter the applicable number of the contract or grant under which the report was written.

8b, 8c, & 8d. PROJECT NUMBER: Enter the appropriate military department identification, such as project number, subproject number, system numbers, task number, etc.

9a. ORIGINATOR'S REPORT NUMBER(S): Enter the official report number by which the document will be identified and controlled by the originating activity. This number must be unique to this report.

9b. OTHER REPORT NUMBER(S): If the report has been assigned any other report numbers *(either by the originator or by the sponsor)*, also enter this number(s).

10. AVAILABILITY/LIMITATION NOTICES: Enter any limitations on further dissemination of the report, other than those imposed by security classification, using standard statements such as:

(1) "Qualified requesters may obtain copies of this report from DDC."

(2) "Foreign announcement and dissemination of this report by DDC is not authorized."

(3) "U. S. Government agencies may obtain copies of this report directly from DDC. Other qualified DDC users shall request through _____."

(4) "U. S. military agencies may obtain copies of this report directly from DDC. Other qualified users shall request through _____."

(5) "All distribution of this report is controlled. Qualified DDC users shall request through _____."

If the report has been furnished to the Office of Technical Services, Department of Commerce, for sale to the public, indicate this fact and enter the price, if known.

11. SUPPLEMENTARY NOTES: Use for additional explanatory notes.

12. SPONSORING MILITARY ACTIVITY: Enter the name of the departmental project office or laboratory sponsoring *(paying for)* the research and development. Include address.

13. ABSTRACT: Enter an abstract giving a brief and factual summary of the document indicative of the report, even though it may also appear elsewhere in the body of the technical report. If additional space is required, a continuation sheet shall be attached.

It is highly desirable that the abstract of classified reports be unclassified. Each paragraph of the abstract shall end with an indication of the military security classification of the information in the paragraph, represented as *(TS), (S), (C), or (U)*.

There is no limitation on the length of the abstract. However, the suggested length is from 150 to 225 words.

14. KEY WORDS: Key words are technically meaningful terms or short phrases that characterize a report and may be used as index entries for cataloging the report. Key words must be selected so that no security classification is required. Identifiers, such as equipment model designation, trade name, military project code name, geographic location, may be used as key words but will be followed by an indication of technical context. The assignment of links, roles, and weights is optional.